Ocean Sci. Discuss., 8, 917–954, 2011
www.ocean-sci-discuss.net/8/917/2011/
doi:10.5194/osd-8-917-2011

Ocean Science Discussions

Development of Black Sea nowcasting and forecasting system

G. K. Korotaev[1], T. Oguz[2], V. L. Dorofeyev[1], S. G. Demyshev[1], A. I. Kubryakov[1], and Y. B. Ratner[1]

[1]Marine Hydrophysical Institute, National Academy of Sciences, Sevastopol, Ukraine
[2]Institute of Marine Sciences, Middle East Technical University, Erdemli, Turkey

Received: 1 March 2011 – Accepted: 1 April 2011 – Published: 27 April 2011

Correspondence to: V. L. Dorofeyev (dorofeyev_viktor@mail.ru)

Published by Copernicus Publications on behalf of the European Geosciences Union.

Abstract

The paper presents the development of the Black Sea community nowcasting and forecasting system under the Black Sea GOOS initiative and the EU framework projects ARENA, ASCABOS and ECOOP. One of the objectives of the Black Sea Global Ocean Observing System project is a promotion of the nowcasting and forecasting system of the Black Sea, in order to implement the operational oceanography in the Black Sea region. The first phase in the realization of this goal was the development of the pilot nowcasting and forecasting system of the Black Sea circulation in the framework of project ARENA funded by the EU. The ARENA project included the implementation of advanced modeling and data assimilation tools for near real time prediction. Further progress in development of the Black Sea nowcasting and forecasting system was made in the frame of ASCABOS project, which was targeted at strengthening the communication system, ensuring flexible and operative infrastructure for data and information exchange between the Black Sea partners and end-users. The improvement of the system was made in the framework of the ECOOP project. As a result it was transformed into a real-time mode operational nowcasting and forecasting system. The paper provides the general description of the main parts of the system: circulation and ecosystem models, data assimilation approaches, the system architecture as well as their qualitative and quantitative calibrations.

1 Introduction

The basis for operational oceanography is the observing system providing regular oceanographic data in real time mode. Operational observations together with modern computers, numerical models and data assimilation methods allow developing the marine environment nowcasting and forecasting. Nowcasting and forecasting of marine environment is similar to the meteorological weather prediction. Integrating structurally different sets of observations which are made available by satellite sensors, moorings, floats and ship-based measurements in the marine nowcasting and forecasting systems allows continuous evolution of the ocean fields in a convenient form with rather high accuracy.

The initiatives for setting up a Black Sea marine nowcasting and forecasting system under the umbrella of the European Commission Framework programmes started with the FP5 ARENA project during the mid-2000s. It is further improved in the FP6 ASCABOS project and transformed into a real-time mode operational system in the ECOOP projects during the second half of the 2000s. The overall goal of ECOOP was to consolidate, integrate and further develop existing European coastal and regional seas operational observing and forecasting systems into an integrated pan-European system. Different basin-scale models mainly resulted from MERSEA system provided initial and boundary conditions for the coastal forecasting. The Black Sea community nowcasting and forecasting system was essential part of the ECOOP. The development and operation system involved a partnership and collaborative efforts of various institutions from the Black Sea riparian states as they joined together in different groups for modelling, observations, data assimilation, data management and serving with limited financial resources. The present form of the Black Sea nowcasting and forecasting system offers a suite of interdisciplinary models and data assimilation schemes that are linked to regional atmospheric model products, and observational sensors mounted on a variety of platforms.

A critical element of this remarkable achievement in a rather short time was a long history of scientific collaboration on the Black Sea oceanographic research. The circulation and ecosystem models were run simultaneously at Marine Hydrophysical Institute (MHI), Ukraine and Institute of Marine Sciences (IMS), Turkey. MHI was also responsible for retrieving satellite data, their processing and assimilation into the models. The meteorological data were provided by the high resolution regional atmospheric model which is fully operational at National Meteorological Administration (NMA) in Romania as a regional implementation of the French global atmospheric model ALADIN. The input data to the oceanic models are collected through Internet or downloaded

OSD
8, 917–954, 2011

from the data base management system. The model products were also stored by the data base management system at IMS. A back up system exists in NIMRD (Romania) which was also responsible to disseminate the forecast products and analyses data to the institutions such as Institute of Oceanology, Bulgarian Academy of Sciences (IO-BAS), Bulgaria, IGF (Georgia), NMA (Romania), Shirshov Institute of Oceanology (SOI), Russia and MHI (Ukraine) to run their high-resolution sub-regional models.

The presented paper consists of the next main parts: description of the Black Sea circulation models used in the nowcasting and forecasting system with schemes of data assimilation; the circulation model calibration; description and calibration of the biogeochemical model; and architecture of the Black Sea nowcasting and forecasting system.

2 Black Sea circulation models and data assimilation approach

Achievements of the operational oceanography during the last decade are considerably connected with significant improvement of the ocean models skill and increase of computers power. Numerical models of the oceanic circulation can be operated now even on personal computers reproducing rather accurately the state of the marine environment and future changes according to the external forcing.

2.1 Description of the circulation models

The Black Sea general circulation models used by the nowcasting and forecasting system are based on the finite-difference approximation of the so-called primitive equations. One of the models is developed by MHI and it is written in the Cartesian coordinate system. The model uses z-coordinate in the vertical direction. It uses Philander-Pacanovsky (Pacanovsky and Philander, 1981) parameterisation of the vertical turbulent viscosity and diffusion. Another model is the implementation of the Princeton Ocean Model (POM), that is also expressed in the Cartesian coordinates in the

OSD
8, 917–954, 2011

horizontal directions and terrain following sigma coordinate in the vertical. The Princeton University model has an advantage with respect to the former one in terms of its more sophisticated parameterization of the turbulent viscosity and diffusion using the Mellor-Yamada 2.5 level turbulence closure (Mellor and Yamada, 1982) that permits a more realistic representation of the surface mixed layer and the sub-surface cold intermediate layer. The horizontal currents, vertical velocity, temperature, salinity and turbulent diffusion coefficients obtained by the POM are used to run the ecosystem model in an offline mode.

Both the MHI model and POM equations are discretized on the C-grid (Arakawa, 1966). The momentum equations in the MHI model are presented in Lamb form (Knysh et al., 2005) which conserves energy and potential enstrophy in the barotropic divergence-free case (Demyshev et al., 1992). The hydrostatic equation in the MHI model allows a more sophisticated representation of nonlinear density dependence from temperature and salinity by admitting exact kinetic and potential energy exchange within a box.

The MHI model has 35 non-uniformly spaced levels which are compressed towards the free surface and the bottom. Horizontal grid resolution is 5 km in both directions that resolves well the mesoscale processes with the Rossby radius of deformation of about 20–25 km in deep part of the Black Sea (Dorofeev et al., 2001). Leap-frog scheme is used for time discretization with periodical switch on of the Matsuno scheme to avoid time slipping feature of the Leapfrog scheme. Vertical coefficients of turbulent viscosity and diffusion were parameterised by Philander-Pakanovsky formula as suggested by Friedrich and Stanev (Friedrich and Stanev, 1988). Horizontal turbulent viscosity coefficient and diffusion coefficient were chosen constant and equal to 5, 10^7 and $5 \times 10^5\, cm^2\, s^{-1}$, respectively.

POM has 7 km horizontal grid step and 26 sigma-levels, which are more frequently near the sea surface and near the bottom. An advantage of the POM model consists of more sophisticated parameterization of the vertical turbulent diffusion and viscosity coefficients. Therefore the results, obtained with the POM model, were used as

OSD
8, 917–954, 2011

input parameters for the Black Sea ecosystem model and for improving the upper layer thermodynamics in the MHI model.

The surface and lateral boundary conditions of the models are provided by the regional atmospheric model, and the climatic data for the river runoffs, water and salt transports through the Kerch and Bosphorus Straits. Surface forcing is an output of the ALADIN atmospheric model of National Meteorological Administration of Romania. ALADIN atmospheric model, the limited area version of the global spectral model ARPEGE/IFS of MeteoFrance, is a tool for the dynamical adaptation and simulation of hydrostatic meso-scale phenomena. It has horizontal space resolution of 24 km and provides 54hours forecast for the Black Sea of wind stress, evaporation and precipitation, sensitive and latent heat flux, long and short wave radiation every 6 hours. Because the Black Sea is a semi-enclosed basin, the lateral boundary conditions are no-slip and zero heat and salt fluxes everywhere except the Bosphorus and Kerch Straits and some major rivers where the temperature and salinity boundary conditions are specific at inflow conditions. Diffusive heat and salt fluxes are set to zero in the straits outflow points.

2.2 Data assimilation approach

Data assimilation is a procedure permitting to combine observations with model simulations for adequate simulation of the marine environment real state (Ghil and Malanotte-Rizzoli, 1991). Operational Black Sea circulation model assimilates real-time satellite altimetry and sea surface temperature.

Sea level anomalies provided by AVISO service were converted into the sea level height (SSH) according to the algorithm described by Korotaev et al. (2001). It is then assimilated into the using the optimal interpolation approach and permits to correct the simulated fields by observations. The correction is performed at the moment of observations and has the following form:

$$\widehat{S}(x,y,z,t) = S(x,y,z,t) + \sum_{n=1}^{N} W_n \cdot [\bar{\varsigma}(x_n,y_n,t) - \varsigma(x_n,y_n,t)] \quad (1)$$

where x,y,z are spatial coordinates, t is time, $S(x,y,z,t)$ is any field which characterises the sea state (below we shall call it as salinity) and is predicted by the model to the moment of observation, $\varsigma(x,y,z,t)$ is the sea level field which is predicted by the model, N is the number of observations of a field ς and $\bar{\varsigma}(x,y,z,t)$ is its observed value. $\widehat{S}(x,y,z,t)$ is the optimal estimation of the field $S(x,y,z,t)$ that takes into account observations of the field $\varsigma(x,y,z,t)$. Weight coefficients W_n are calculated through the cross-covariance function $P^{S\varsigma}$ of errors of salinity S and sea level ς forecast and the auto-covariance function $P^{\varsigma\varsigma}$ of errors of the field ς (Knysh et al., 1996).

Let us present error covariance functions in the form

$$P^{S\varsigma}(x,y,z,x',y',t) = \sigma^S(x,y,z,t) \cdot \sigma^{\varsigma}(x',y',t) \cdot \bar{P}^{S\varsigma}(x,y,z,x',y',t) \quad (2)$$

$$P^{\varsigma\varsigma}(x,y,x',y',t) = \sigma^{\varsigma}(x,y,t) \cdot \sigma^{\varsigma}(x',y',t) \cdot \bar{P}^{\varsigma\varsigma}(x,y,x',y',t) \quad (3)$$

where $\sigma^S(x,y,t)$ and $\sigma^{\varsigma}(x,y,t)$ are standard deviations of errors of salinity and sea level predictions, respectively, $\bar{P}^{S\varsigma}$ is the cross-correlation function of errors of the sea level and salinity fields and $\bar{P}^{\varsigma\varsigma}$ is auto-correlation function of errors of the sea level. Let the following assumptions:

1. Errors of the predicted fields are stationary in time as well as horizontally uniform and isotropic. Then

$$\sigma^S = \sigma^S(z) \quad (4)$$

$$\sigma^{\varsigma} = \text{const} \quad (5)$$

$$\bar{P}^{S\varsigma} = \bar{P}^{S\varsigma}(r,z) \quad (6)$$

OSD
8, 917–954, 2011

$$\bar{P}^{\varsigma\varsigma} = \bar{P}^{\varsigma\varsigma}(r) \quad (7)$$

where $r^2 = (x-x')^2 + (y-y')^2$.

2. Cross-correlation between salinity and sea level is presented as a product of two factors:

$$\bar{P}^{S\varsigma}(r,z) = \bar{P}^{S\varsigma}(r) \cdot \bar{P}^{S\varsigma}(z) \quad (8)$$

3. A statistic of errors of the predicted fields is proportional to the natural statistics of the same fields.

Under these assumptions, the variance, auto-correlation and cross-correlation functions estimated from observations are used in the simulations. Normalized weight coefficients for the temperature and salinity fields are presented on Fig. 1.

Sea surface temperature (SST) retrieved from NOAA AVHRR data was assimilated in the model. Reception and pre-processing of AVHRR data was carried out by MHI group. SST retrieved from AVHRR measurements on 1 km grid was interpolated then on the model grid. The assimilation of SST derived from AVHRR sensors was carried out by replacing the simulated temperature within the upper mixed layer by the observed SST. The mixed layer depth was determined by combining the simulated temperature and salinity profiles analysis and Obukhov's formula (Obukhov, 1946), which follows from the turbulent energy balance. Bearing in mind that the cloudiness is impenetrable for IR radiation and some gaps can appear on SST maps derived from AVHRR data. Therefore, the observed SST is optimally interpolated using the SST prediction as a base. Then interpolated values are assimilated as it was explained above. Such approach permits to avoid artificial fronts on the simulated SST maps.

SST and SSH assimilation permits to keep the surface layer thermodynamics and topography of permanent pycnocline close enough to the real state. However operational observations in the Black Sea do not cover the deep layers of the basin with required density. Profiling floats observations are too rare and only special approach elaborated last time (Demyshev et al., 2010) should permit to assimilate them. An assimilation of the temperature and salinity profiles obtained by averaging of the climatic arrays over the basin area was used in the model which operated during ECOOP project. This method has significant drawback as the climatic profiles are unable to trace decadal variability of vertical stratification. Nevertheless assimilation of the climatic profiles make possible to prevent slow sliding of the model to its own climate.

3 Circulation model calibration

The circulation models have been subject to extensive set of qualitative and quantitative tests prior to the operational phase. Next two subsections present some of those tests to show the model ability to reproduce major characteristics of the Black Sea dynamics and important features of the temperature and salinity stratification.

3.1 Qualitative model calibration

The Black Sea circulation model was first calibrated by the climatological data. The attention was focused particularly on reproduction of the Black Sea Rim Current and its seasonal variability as well as main coastal anticyclonic eddies (e.g. Batumi gyre). Analysis of the model salinity has to show that the model simulates the Other specific features for the model calibration are the reproduction of the main halocline, the seasonal thermocline, salinity decrease from the basin center to its periphery. It is necessary to evaluate the model possibility to reproduce the cold intermediate layer (CIL), its reproduction sites and two mechanisms of formation (e.g. winter convection in the central part of the basin and subduction of cold waters from the northwestern shelf).

An example of the Black Sea surface topography evolution during April 2003 is shown on Fig. 2. The strong gradient around the periphery corresponds to the Rim Current jet, its contours are streamlines of the surface geostrophic currents; thus, closed contours represent mesoscale eddies. The overall circulation system shown in Fig. 2 therefore

OSD
8, 917–954, 2011

possesses the meandering Rim Current system cyclonically encircling the basin and a set of coastally-attached anticyclonic eddies around the basin, the most notable of which are the Bosphorus, Batumi, Sukhumi, Caucasus, Kerch, Sevastopol, and Constantsa anticyclonic eddies on the coastal side of the Rim Current zone. The Batumi anticyclone is present in the south-eastern corner of the basin as the most intense and persistent of the Black Sea coastal eddies. The Rim Current structure is shown also on Fig. 3.

The maps of temperature distribution on the 50 m depth reveal a complex picture of spatial variability caused by shear currents (Fig. 4). For example, Fig. 4a shows relatively warm and salty Mediterranean water injected by the Mediterranean underflow near the northern exit of the Bosphorus Strait and its subsequent distribution by currents. It appears to be an intermittent feature depending on the character of large scale circulation features near the strait. Small lenses of warm water similar to "meddies" in the Atlantic Ocean near the Gibraltar strait are formed near the Bosphorus mouth and then transported by Rim current. Such warm lens is seen in Fig. 4a in the southeast corner of the basin. Such features have not been documented and yet to be confirmed by observations.

Figure 4b shows subduction of cold waters (dark color) from the northwest shelf to the deep sea. In the same figure the set mushroom-like structures also is visible near the northwest shelf of the sea, in the southwestern corner of basin just opposite to a mouth of the Bosporus Strait and along the Anatolian coast. Usually such mushroom-like structures are observed on the sea surface on satellite images, but rarely captured by direct observations that require high resolution synoptic sampling at the right time and location.

Figure 5 presents distribution of salinity anomalies at 105 m during September 1995. Light colors correspond to the salinity lower than basin-average value, and vise-versa for dark colors. Eddies of different signs are presented in deep waters according to Fig. 5. Low salinity water is preferentially observed in the coastal anticyclonic eddies, whereas more salty water is observed in cyclonic gyres of the interior basin. As

OSD
8, 917–954, 2011

documentred previously (Korotaev et al., 2001, 2003), the Rim current is relatively weak in the summer and fall seasons and the basin acquires more turbulent flow structure of mesoscale eddies as also supported by Fig. 5.

The vertical section of water temperature along 42.7° N is presented on Fig. 6. It illustrates a typical vertical structure of the temperature in the Black Sea. The mixed layer occupies the upper 25 m. The water temperature decreases below the upper mixed layer forming a seasonal thermocline. The cold intermediate layer (CIL), which is a specific feature of the Black Seas thermal stratification, occupies the layer between 50 and 80 m depth (violet colour on Fig. 6). The temperature grows below the CIL down to the bottom.

The Rim current frontal zone can be clearly seen in the left part of the section. The deepening of the thermocline as well as the Rim current jet is attached to the bottom slope. Thus the simulated fields are in a good qualitative agreement with observations. General features of the basin dynamics and stratification are well presented by model results.

3.2 Quantitative model calibration

Quantitative calibration of the simulated fields is an essential part of the Black Sea forecasting system development. This calibration is carried out with use of regular space remote sensing measurements, in situ data of hydrographic surveys, surface drifting buoys and deep profiling floats.

3.2.1 Hydrographic surveys and profiling floats

Initial tuning of the basin-scale circulation model was made against the data of four large-scale hydrographic ComsBlack surveys which were fulfilled in 1992–1995 yr (Oguz et al., 1993). The model was run without assimilation of SST. ComsBlack hydrography was used to estimate quantitatively the accuracy of 3-D temperature and salinity field simulations. Standard deviations of simulated fields against the observed

Discussion Paper | Discussion Paper | Discussion Paper | Discussion Paper |

OSD

8, 917–954, 2011

Development of Black Sea nowcasting and forecasting system

G. K. Korotaev et al.

ones were calculated on each depth level (Dorofeyev and Korotaev, 2004a). These functions are presented on Fig. 7. The standard deviation of the model analysis is compared with the natural variability of the temperature and salinity fields, i.e. with the standard deviation of the climatic data against observations.

Figure 7 shows, that the altimetry assimilation brings the most significant improvement in salinity field. It is natural, because density stratification in the Black Sea depends mainly on salinity. Assimilation of altimetry allows describing about 25% of the salinity natural variability within the halocline where the difference between simulated and measured fields is the most significant. In the regions of high vertical gradients even small error in the isohaline depth produces large error. However simulated salinity maps agree well with observations, as it was shown earlier by Dorofeyev and Korotaev (2004a).

Standard deviation of temperature is the largest near the surface (here the error is greater than in the case of comparison with buoy data). It means that the thermodynamics of the top sea layer in the model is too simplified. An explicit description of the mixed layer dynamics is necessary to include for better reproduction of surface temperature by the model. Additional extremes of the temperature standard deviation are observed near the thermocline and within CIL. Increase of the error near the thermocline has the same reason, as in the case of salinity.

The correlation coefficients of simulated and observed fields of temperature and salinity are large enough. The highest correlation for both fields occurs within the pycnocline with approximately 0.65 for salinity and 0.45 for temperature.

The comparison of the model output with ComsBlack hydrography has shown reasonable consistency of the simulations against observations in deep layers of the basin and further points to the importance of SST assimilation.

3.2.2 SST calibration

The model runs with SST assimilation were compared with the daily averaged simulations with similar data of surface drifters. It is shown (Ratner and Bayankina, 2004)

OSD
8, 917–954, 2011

that the standard deviation is in the range 0.5–0.7° (i.e. it is in the same range as the accuracy of SST retrieving from AVHRR data). Thus, assimilation of SST retrieved from IR observations improves significantly the accuracy of the mixed layer temperature. However the consistency of simulated and observed mixed layer depth depends on the quality of the upper layer thermodynamics in the model.

3.2.3 Drifters with thermistor chain

Quality of the products of the upper layer thermodynamics is improved by comparing the simulated temperature profiles in the upper 70 m layer with direct measurements by the surface drifting buoys with thermistor chain. Careful tuning of the Phylander-Pakanovsky approximation to the Black Sea conditions was done by Demyshev (Demyshev et al., 2009). Improved version of the circulation model provides reasonable description of both shoaling and deepening of the mixed layer (Figs. 8 and 9).

3.2.4 Profiling floats

Temperature and salinity profiles are also compared with data provided by profiling floats. Figure 10 demonstrates the standard deviations for temperature and salinity fields, which are similar to those obtained by using earlier by the ComsBlack surveys (Dorofeev and Korotaev, 2004b).

3.2.5 Surface velocity

Comparison of several drifting buoys trajectories with the simulated surface currents in January 2002 is presented in Fig. 11. Trajectories are computed from the buoy coordinates during three days and the simulated currents at mid-days in the figure. For example, the trajectories of the buoy numbers 7 and 14 were under the influence of Rim Current. Buoy number 14 has been captured by the current for almost a month starting from 15–16 January 2002. We note its circular motion near the cape Sinop as inferred from its trajectories during 23 and 31 January. Buoy number 7 also has been captured by the stream of Rim Current on 23 January. It moved along the offshore side of the jet and has practically left the current on February 2002 and picked up again as they move eastward along the coast of Turkey. The buoy number 17 was located in the open part of the sea during the same period and was transported on the east by mesoscale jets periodically produced as clearly seen on 31 January in Fig. 11.

The trajectory of the buoy number 8 in Fig. 11 illustrates an accuracy of coastal currents simulations. The drift of buoy number 8 during 15–31 January well corresponds to the model simulated narrow coastal jet in the northeast direction in the vicinity of cape Kaliakra of the Bulgarian coast. A small branch of the jet has transported the buoy number 8 towards the shore on 31 January where it remained up to the mid of February 2004. More examples of buoys trajectories are presented in Korotaev et al. (2004). The evolution of current velocity along the trajectory of drifting buoy also demonstrates good reproduction of the low-frequency flow variability by the model (Korotaev et al., 2004).

The quantitative comparison of the daily averaged surface current velocity and simulations shown on Fig. 12 for zonal and meridional components indicates that the simulated velocity components are systematically underestimated by the model. This may be resulted from the different spatial averaging of the signal. Drifting buoys measure currents along a line whereas the model simulated velocity is averaged in the box 5×5 km. High resolution surface current maps obtained by means of the imagery processing (Korotaev et al., 2008) show that the Rim current has fine structure in the form of narrow and intense submesoscale jets. However the current grid size of the model (5 km) is able to resolve mesoscale eddies but not submesoscale structures. Future improvement of the Black Sea operational model should include explicit representation of submesoscale features.

Surface drifting buoys with data transmission via IRIDIUM provide a possibility to validate high-frequency variability of surface currents. IRIDIUM data transmission allows to determine buoy coordinates often enough to describe trajectory loops related to the inertial oscillations. The comparison of measured and simulated current velocity

OSD
8, 917–954, 2011

oscillations at inertial frequency (Fig. 13) shows that they can strongly disturb instant surface current velocity. The model often reproduces the phase of inertial oscillations whereas their amplitude usually is underestimated. Evidently, the accuracy of the inertial oscillation simulations depends strongly on the quality of atmospheric forcing.

3.2.6 Deep velocity

Data of profiling floats allow evaluation of the weekly averaged deep velocity accuracy. In general, relative accuracy of the current speed simulation by the model is highest on the depth 200 m. However weekly mean currents even on the depth 1550 m measured by profiling float and simulated by the model are in good consistency (Dorofeev and Korotaev, 2004b).

4 Ecosystem model

The main part of the Black Sea ecosystem model is a biogeochemical model. The 3-D biogeochemical model coupled with the circulation model is based on the one given by Oguz et al. (2001). It has one-way coupling with circulation model through current velocity, temperature, salinity and turbulent diffusivity. The biogeochemical model extends to 150 m depth with 15 z-levels, compressed to the sea surface. It includes 9 state variables. Phytoplankton is represented by two groups, typifying diatoms and flagellates. Zooplankton is also separated into two groups: microzooplankton (nominally <0.2 mm) and mesozooplankton (0.2–2 mm). The trophic structure includes also nonphotosynthetic free living bacteriaplankton, detritus and dissolved organic nitrogen. Nitrogen cycling is resolved into two inorganic forms: nitrate and ammonium. Nitrogen is considered as the only limiting nutrients for phytoplankton growth. So, all these variables are presented in the model equations in units of mmol N m^{-3}. The local temporal variations of all variables are expressed by equations of the general form

OSD
8, 917–954, 2011

$$\frac{\partial F}{\partial t} + \frac{\partial (uF)}{\partial x} + \frac{\partial (vF)}{\partial y} + \frac{\partial ((w+w_s)F)}{\partial z} = K_h \nabla^2 F + \frac{\partial}{\partial z}(K_v \frac{\partial F}{\partial z}) + \Re(F), \tag{9}$$

where $\Re(F)$ is the interaction term, which expresses a balance of sources and sinks of each of biological and geochemical variables F; w_s represents the sinking velocity for diatoms and detrital material and is set to zero for other compartments; (u, v, w) – components of the current velocity, K_h, K_v – horizontal and vertical coefficients of turbulent diffusion. The last parameters are provided by physical model (the circulation model). Space resolution for the both parts of the ecosystem model (physical and biogeochemical) is approximately 5 km.

Fluxes of all biogeochemical variables are set to zero on the sea surface, bottom in shallow part of the basin and on the lateral boundaries, except river estuaries, where nitrate fluxes are set up proportional to rivers discharges and nitrate concentrations. On the lower liquid boundary in the deep part of the basin concentrations of all parameters set to zero except ammonium and hydrogen sulfide (sulfide and ammonium pools).

5 Calibration of the ecosystem model

The model reproduces reasonably well the seasonal cycling of phytoplankton and other biochemical fields (Fig. 14). Concentration of nitrate increases during the winter mixing period and reduces to zero after the spring bloom of phytoplankton. The spring bloom of phytoplankton is well presented on the central panel of the figure. It shows also the secondary subsurface maximum of phytoplankton on the bottom of the summer and autumn bloom. The distribution of zooplankton follows closely that of phytoplankton with a time lag of approximately half a month.

Numerical simulations of the Black Sea ecosystem with 5 km grid step demonstrate its ability reproducing large scale spatial features and reaction on the mesoscale dynamics. Figure 15 shows the snapshot of the surface phytoplankton distribution during mid-August 1998 resulted from simulations (right panel) and chlorophyll-*a* concentration according to SeaWiFS measurements. There is rather good consistency between these two fields. such as broad area of high phytoplankton concentration on the North-West shelf of the Black Sea, the strip of increased values along the western and southern coasts of the basin until the Sinop cape, and large filaments near the western coast of the basin (across the Kaliakra cape) induced by the mesoscale anticyclonic eddy propagating along the shelf break.

6 Architecture of the nowcasting and forecasting system

A pilot version of the Black Sea nowcasting/forecasting system (Korotaev et al., 2006) was built in the framework of FP5 ARENA project. It operated during five days in July 2005 in the manual mode. The system architecture was improved significantly during the next years to avoid manual operation. During ECOOP project phase it operated in real time mode. It forms version V0 of the model currently used in the My Ocean Black Sea Marine Forecasting Centre.

The software controlling the system is presented by three groups. The group of input and pre-processing consists of three sub-groups: ALTIMETRY, NOAASST and METEO. The sub-group ALTIMETRY includes downloading of SLA of missions Topex/Poseidon, ERS-2, Jason-1, Envisat and GFO from the web of AVISO centre and its pre-processing according to the algorithm described in Korotaev et al. (2001). The sub-group NOAASST is assigned to the pre-processing of IR/AVHRR data received by the HRPT station at MHI to retrieve the SST. The sub-group METEO includes downloading of meteorological analysis and forecast of the sea surface wind, heat fluxes and precipitation/evaporation from the web of NMA (Romania) and their repacking. The group MHI-casting consists of the collection of software for the numerical process control. It provides numerical simulation of the Black Sea circulation, data assimilation in the circulation model and simulation of the surface wave field. The group of the output includes three sub-groups ARCH, GRAF and NET for the data archiving, graphic presentation of the system products and data distribution via Internet.

OSD
8, 917–954, 2011

The scheme of the data flow is presented on Fig. 16. The output of the system is three dimensional temperature, salinity and current velocity fields. Products of the system on the sea surface were regularly presented on the web site http://dvs.net.ua/mp as images and in digital form. Examples of the system products presented on the web are shown on Fig. 17.

7 Conclusions

The pilot version of the Black Sea nowcasting and forecasting system which was built in the framework of the FP 5 ARENA and FP6 ASCABOS projects was significantly improved later during the FP6 ECOOP project. The basin-scale forecasting became operational in the real-time mode from the beginning of the ECOOP project and served as mainframe system for further development of the operational coastal forecasting systems in the Black Sea. Started from "V0 version" it was upgraded to the Black Sea GOOS system "V2". This last version consists of a regional system, covering the entire Black Sea area, and 3 sub-regional systems covering respectively: the North Western shelf, the Bosphorus and Western shelf, and the South coast of Crimea and North East Black sea. The paper was targeted at the description of development of the basin-wide nowcasting and forecasting system. The circulation model, which is the core of the system, was improved during the ECOOP by including a new parameterization of the vertical mixing processes. In addition it was added with the biogeochemical model. Together with the circulation model it allows describing evolution of the Black Sea ecosystem. The models have been subject to the qualitative and quantitative tests, which are the essential part of the system. Archive climatic, hydrographical surveys data and measurements from the drifter and profiling floats were used for the models calibrations. Calibration tests showed reasonable accuracy of the system products. The system architecture was improved significantly to avoid manual operation and during ECOOP project phase it operated in real time mode. The operational system established during ECOOP is the V0 version of the basin-wide nowcating and forecasting system in the frame of the FP7 My Ocean project.

OSD
8, 917–954, 2011

Acknowledgements. The research leading to the results has received funding from the European Community's Sixth Framework Programme under the grant agreement No 036355 (ECOOP).

References

Arakawa, A.: Computational design for long-term numerical integration of the equations of fluid motion: Two-dimensional incompressible flow. Part I, J. Comput. Phys., 1, 119–43, 1966.

Demyshev, S. G. and Korotaev, G. K.: Numerical energy-balanced model of baroclinic currents in the ocean with bottom topography on the C-grid, in: Numerical models and results of intercalibration simulations in the Atlantic ocean, Moscow, 163–231, 1992 (in Russian).

Demyshev, S. G., Dovgaya, S. V., and Markova, N. V.: Numerical simulations of hydrophysical fields of the Black Sea from January to September 2006, Ecological Security of Coastal and Shelf Zone and Complex use of Shelf Resources, 19, 355–369, 2009 (in Russian).

Demyshev, S., Knysh, V., Korotaev, G., Kubryakov, A., and Mizyuk, A.: The MyOcean Black Sea from a scientific point of view, Mercator Ocean Newsletter, 39, 16–24 October, available at: http://www.mercator-ocean.fr/documents/lettre/lettre_39_en.pdf, 2010.

Dorofeyev, V. L. and Korotaev, G. K.: Assimilation of the satellite altimetry data in the eddy-resolving model of the Black Sea circulation, Marine Hydrophys. Journ., 1, 52–68, 2004a (in Russian).

Dorofeyev, V. L. and Korotaev, G. K.: Validation of the results of modeling the Black Sea circulation based on the data of floating buoys, Ecological Security of Coastal and Shelf Zone and Complex use of Shelf Resources, 11, 63–74, 2004b (in Russian).

Dorofeyev, V. L., Demyshev, S. G., and Korotaev, G. K.: Eddy-resolving model of the Black Sea circulation, Ecological Security of Coastal and Shelf Zone and Complex use of Shelf Resources, 71–82, 2001 (in Russian).

Friedrich, H. J. and Stànev, E. V.: Parameterization of vertical diffusionin numerical model of the Black Sea, Small sea turbulence and mixing in the ocean, Elsev. Oceanogr. Serie., 46, 151–167, 1988.

Ghill, M. and Malanotte-Rizzoli, P.: Data assimilation in meteorology and oceanography, in: Advances in Geophysics, edited by: Saltzmann, B., Academic Press, 33, 141–266, 1991.

Knysh, V. V., Saenko, O. A., and Sarkisyan, A. S.: Method of assimilation of altimeter data and its test in the tropical North Atlantic, Russ. J. Numer. Anal. M., 11(5), 333–409, 1996.
Knysh, V. V., Kubryakov, A. I., Inyushina, N. V., and Korotaev, G. K.: Reconstruction of the climatic seasonal Black Sea circulation by means of sigma-coordinate model and assimilation of the temperature and salinity data, Ecological safety of coastal and shelf zone and complex use of their resources, Sevastopol, 12, 243–265, 2005 (in Russian).
Korotaev, G. K., Saenko, O. A., and Koblinsky, C. J.: Satellite altimetry observations of the Black Sea level, J. Geophys. Res., 106(C1), 917–933, 2001.
Korotaev, G. K., Oguz, T., Nikiforov, A. A., and Koblinsky, C. J.: Seasonal, interannual and mesoscale variability of the Black Sea upper layer circulation derived from altimeter data, J. Geophys. Res., 108(C4), 3122, doi:10.1029/2002JC001508, 2003.
Korotaev, G. K., Dorofeyev, V. L., and Smirnova, T. Yu.: Accuracy of the diagnosis of surface currents in the system of the Black Sea satellite monitoring, Ecological Security of Coastal and Shelf Zone and Complex use of Shelf Resources, 11, 75–92, 2004 (in Russian).
Korotaev, G. K., Cordoneanu, E., Dorofeyev, V. L, Fomin, V., Grigoriev, A. V., Kordzadze, A. Kubryakov, A. I., and Oguz, T.: Near-operational Black Sea nowcasting/forecasting system, in: European Operational Oceanography: Present and Future, 4th EuroGOOS Conference, 6–9 June 2005, Brest, France, 2006.
Korotaev, G. K., Huot, E., Le Dimet, F.-X., Herlin, I., Stanichny, S. V., Solovyev, D. M., and Wu, L.: Retrieving ocean surface current by 4-D variational assimilation of sea surface temperature images, Remote Sens. Environ., 112(4), 1464–1475, 2008.
Mellor, G. L. and Yamada, T.: Development of a turbulence closure model for geophysical fluid problems, Rev. Geophys. Space Ge., 20, 851–875, 1982.
Obukhov, A. M.: Turbulence in temperature heterogeneous atmosphere, Proceedings of Institution of Theoretical Physics SU Academy of Science, 24(151), 3–42, 1946.
Oguz, T., Latun, V. S., Latif, M. A., Vladimirov, V. V., Sur, H. I., Makarov, A. A., Ozsoy, E., Kotovshchikov, B. B., Eremeev, V., and Unluata, U.: Circulation in the surface and intermediate layers of the Black Sea, Deep-Sea Res. Pt. I, 40, 1597–1612, 1993.
Oguz, T., Ducklow, H. W., Malanotte-Rizzoli, P., Murray, J. W., Shushkina, E. A., Vedernikov, V. I., and Unluata, U.: A physical-biochemical model of plankton productivity and nitrogen cycling in the Black Sea, Deep-Sea Res. Pt. I, 46(4), 597–636, 1999.
Oguz, T., Ducklow, H. W., and Malanotte-Rizzoli, P.: Modeling distinct vertical biochemical structure of the Black Sea: Dynamical coupling of the oxic, suboxic, and anoxic layers, Global

Biochem. Cy., 14(4), 1331–1352, 2000.
Oguz, T., Ducklow, H. W., Purcell, J. E., and Malanotte-Rizzoli, P.: Modeling the response of top-down control exerted by gelatinous carnivores on the Black Sea pelagic food web, J. Geophys. Res, 106(C3), 4543–4564, 2001.
Pacanovsky, R. C. and Philander, G.: Parameterization of vertical mixing in numerical models of the tropical ocean, J. Phys. Oceanogr., 11, 1442–1451, 1981.
Ratner, Yu. B. and Bayankina, T. M.: Comparison of the surface temperature values obtained from the model of the Black Sea dynamics and the data of SVP-drifters in March–August 2003, Ecological Security of Coastal and Shelf Zone and Complex use of Shelf Resources, 11, 51–62, 2004 (in Russian).

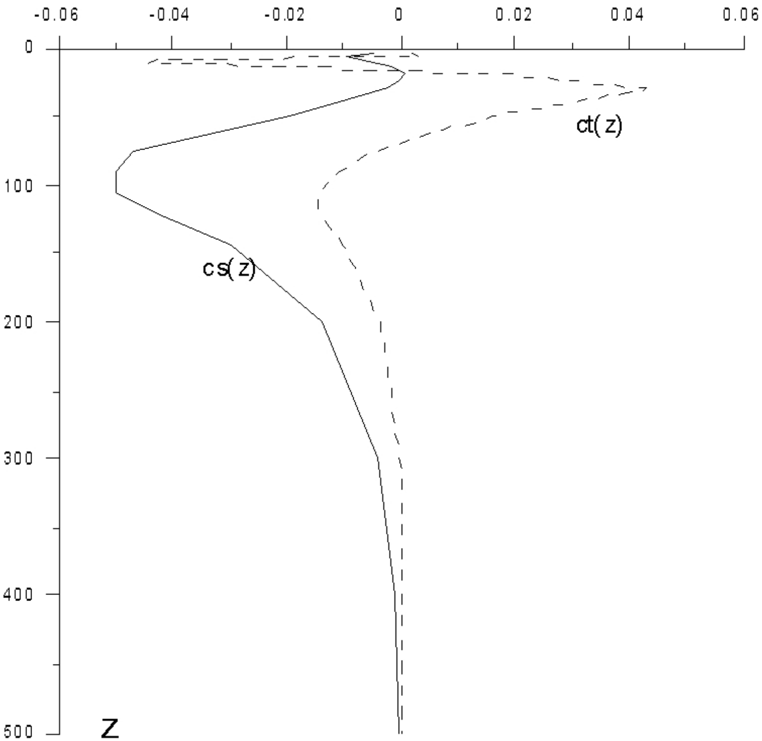

Fig. 1. Normalized weight coefficients for extrapolation of temperature and salinity with depth.

OSD

8, 917–954, 2011

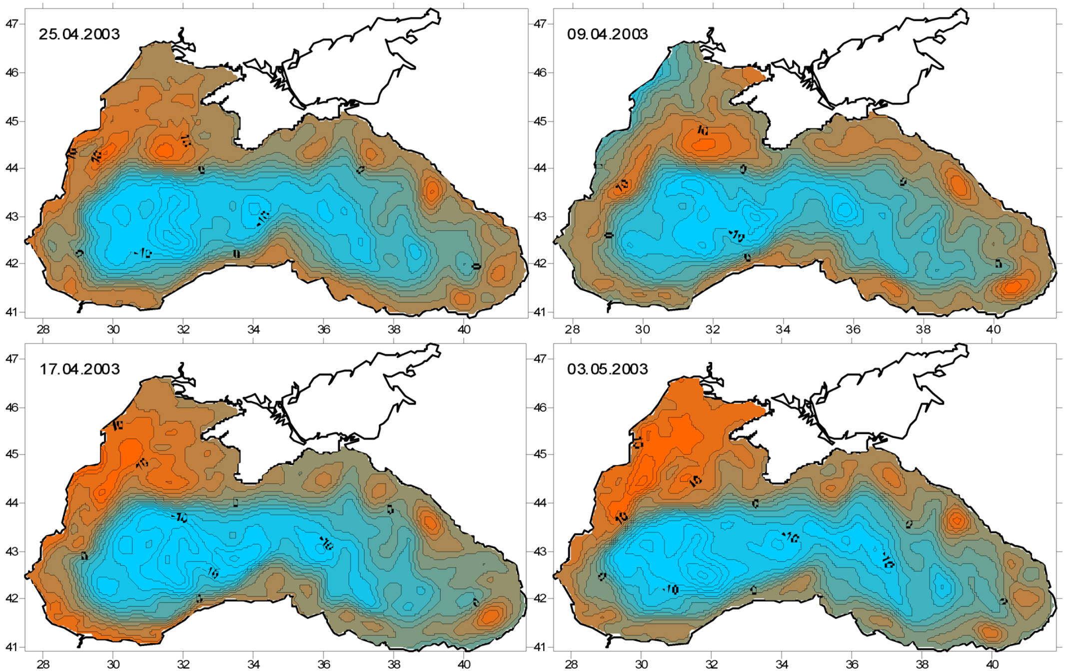

Fig. 2. Short-term evolution of the sea surface topography.

OSD

8, 917–954, 2011

Development of Black Sea nowcasting and forecasting system

G. K. Korotaev et al.

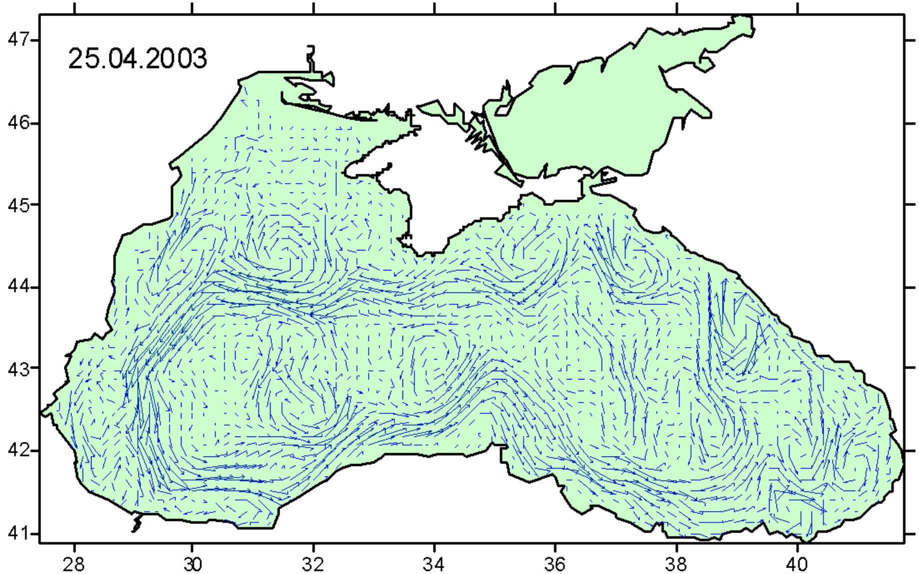

Fig. 3. Surface circulation in spring season simulated by the model.

OSD
8, 917–954, 2011

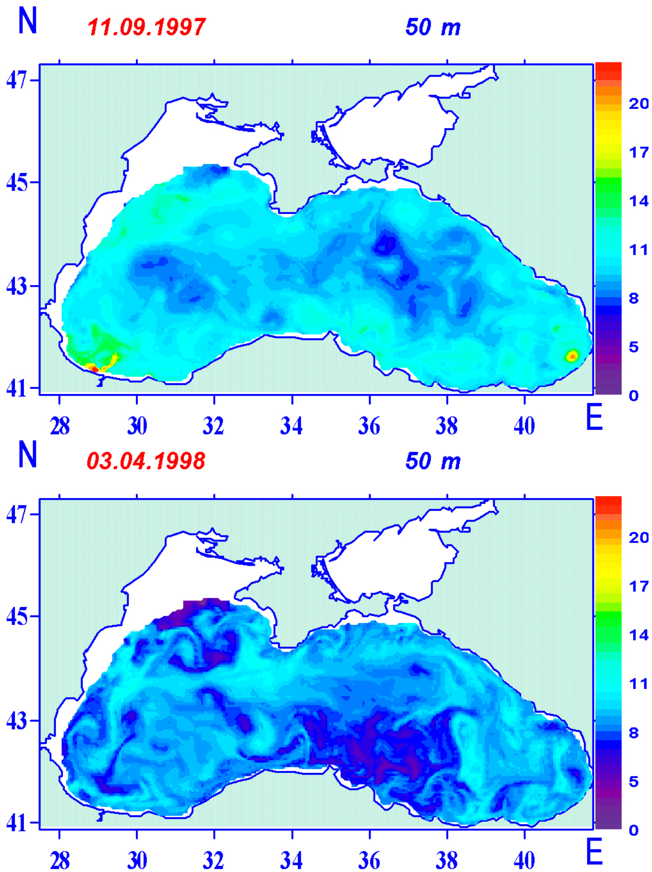

Fig. 4. Temperature distribution on the depth 50 m.

OSD

8, 917–954, 2011

Development of Black Sea nowcasting and forecasting system

G. K. Korotaev et al.

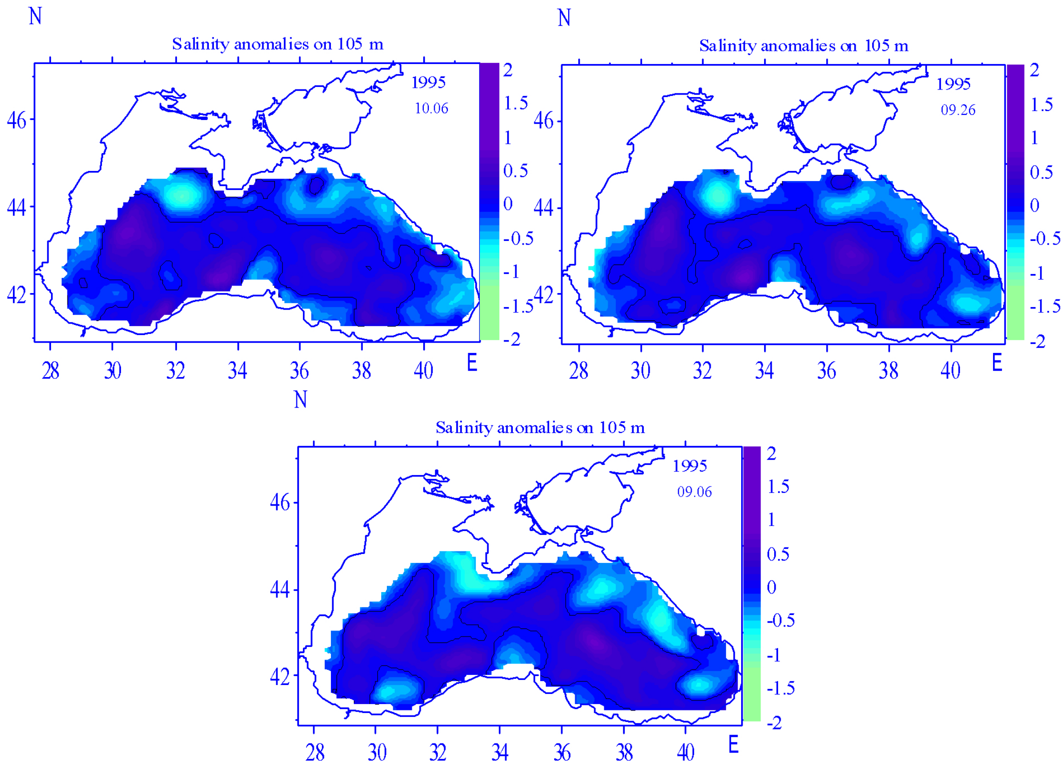

Fig. 5. Salinity anomaly on the depth 105 m.

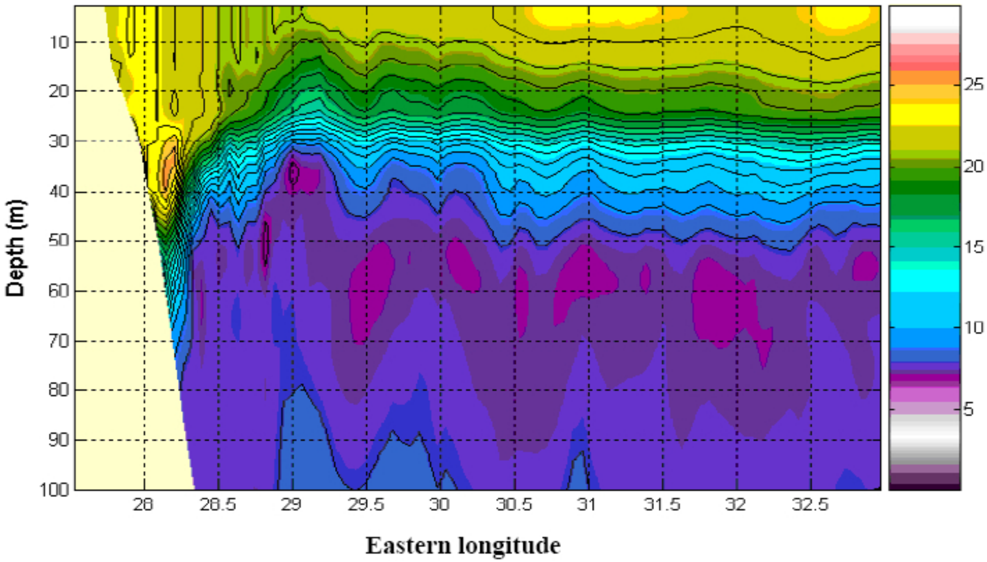

Fig. 6. Temperature section along 42.7° N in the upper 100 m on 29 September 2005. Contour interval is equal to 1 °C. The lowest and the next isotherms correspond to 8 °C and bound the CIL section.

OSD
8, 917–954, 2011

Development of Black Sea nowcasting and forecasting system

G. K. Korotaev et al.

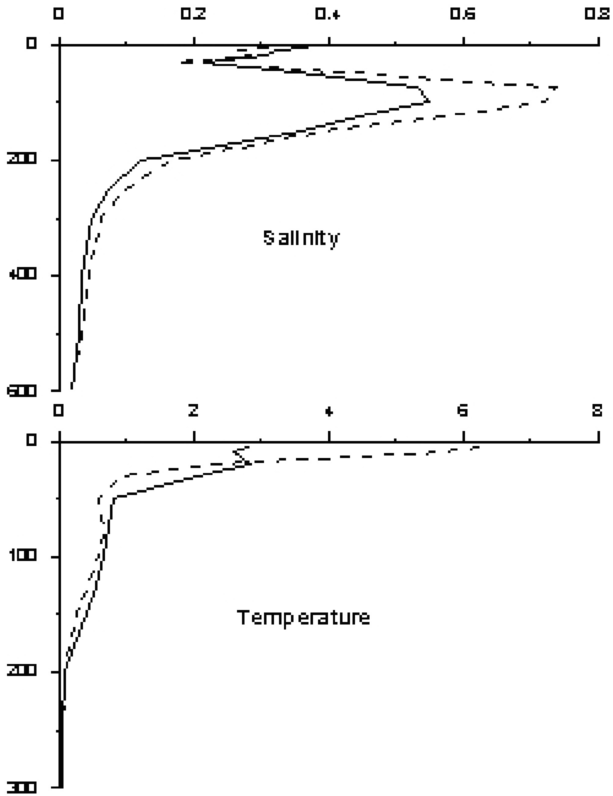

Fig. 7. Standard deviation of the differences between simulated and observed fields as a function of depth (solid lines), and the natural variability (root mean square deviation from mean value) of the same fields (dash lines) (according to Dorofeyev and Korotaev, 2004a).

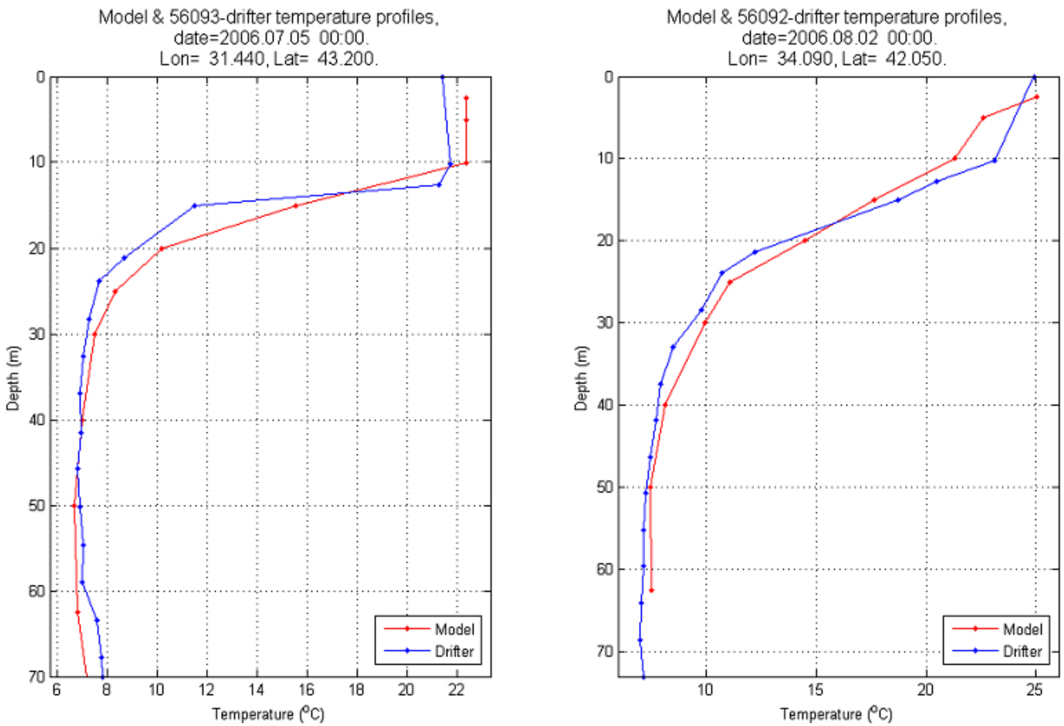

Fig. 8. Comparison of the simulated (blue line) and measured (red line) temperature profiles in the upper 70 m during the shoaling of the mixed layer.

OSD
8, 917–954, 2011

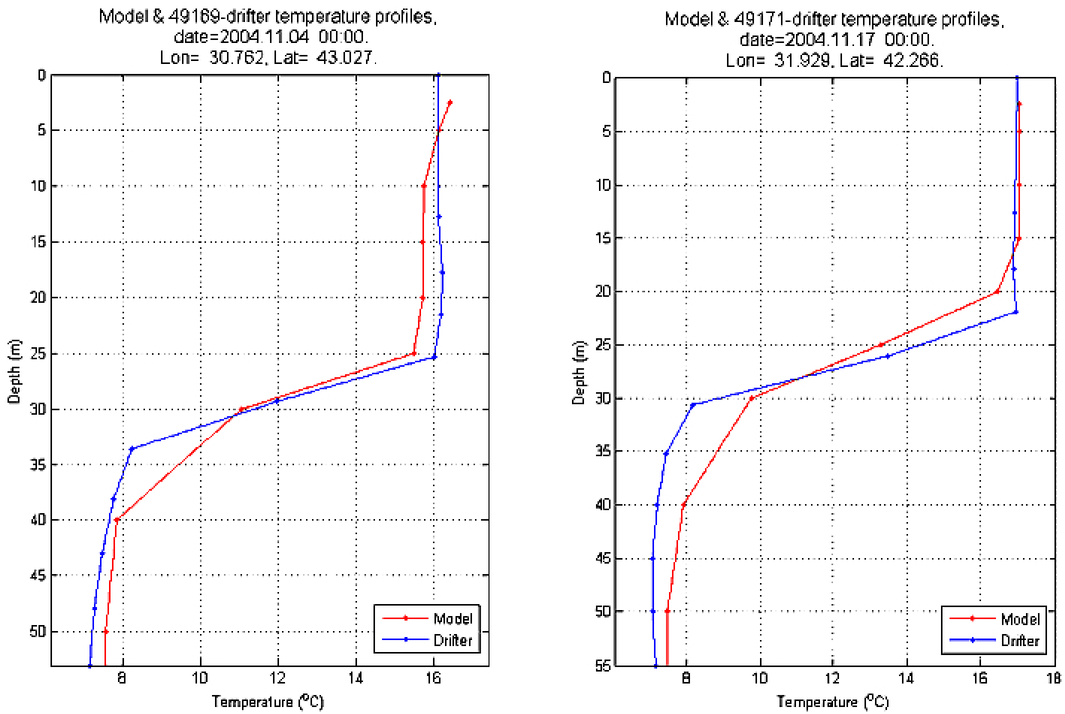

Fig. 9. Comparison of the simulated (blue line) and measured (red line) temperature profiles in the upper 70 m during the deepening of the mixed layer.

OSD
8, 917–954, 2011

Development of Black Sea nowcasting and forecasting system

G. K. Korotaev et al.

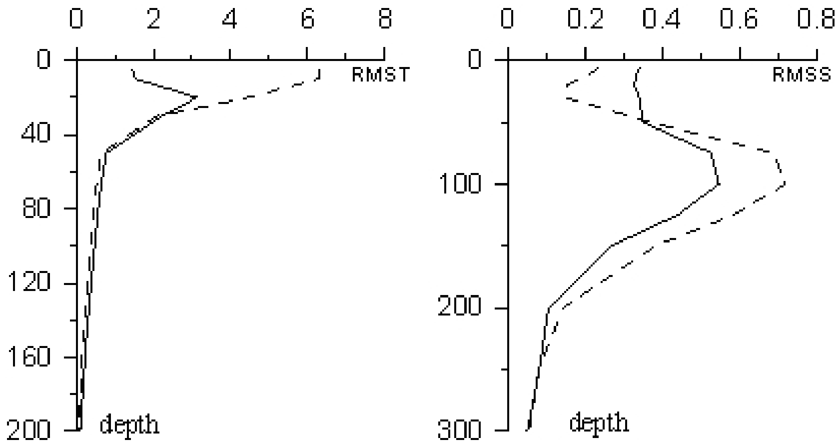

Fig. 10. Standard deviation of the differences between simulated and measured fields as a function of depth (solid lines), and the natural variability of the same fields (dash lines).

OSD
8, 917–954, 2011

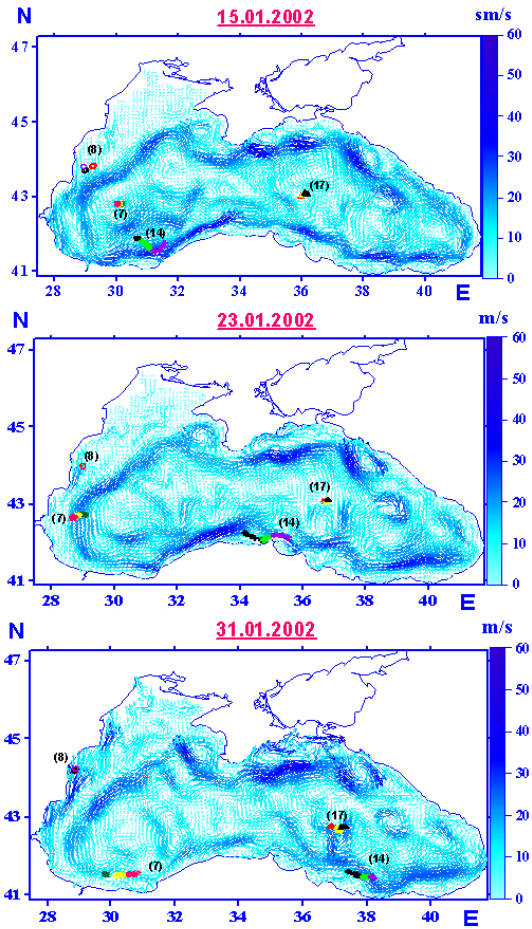

Fig. 11. Trajectories of surface drifting buoys overlapped on the simulated circulation. January 2002.

OSD
8, 917–954, 2011

Development of Black Sea nowcasting and forecasting system

G. K. Korotaev et al.

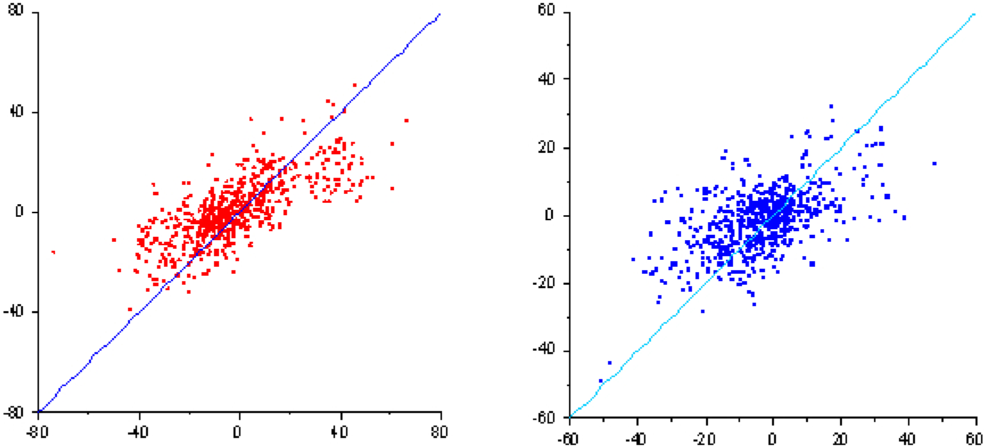

Fig. 12. Scatter plot of the simulated (vertical axe) and observed (horizontal axe) surface currents.

OSD

8, 917–954, 2011

Development of Black Sea nowcasting and forecasting system

G. K. Korotaev et al.

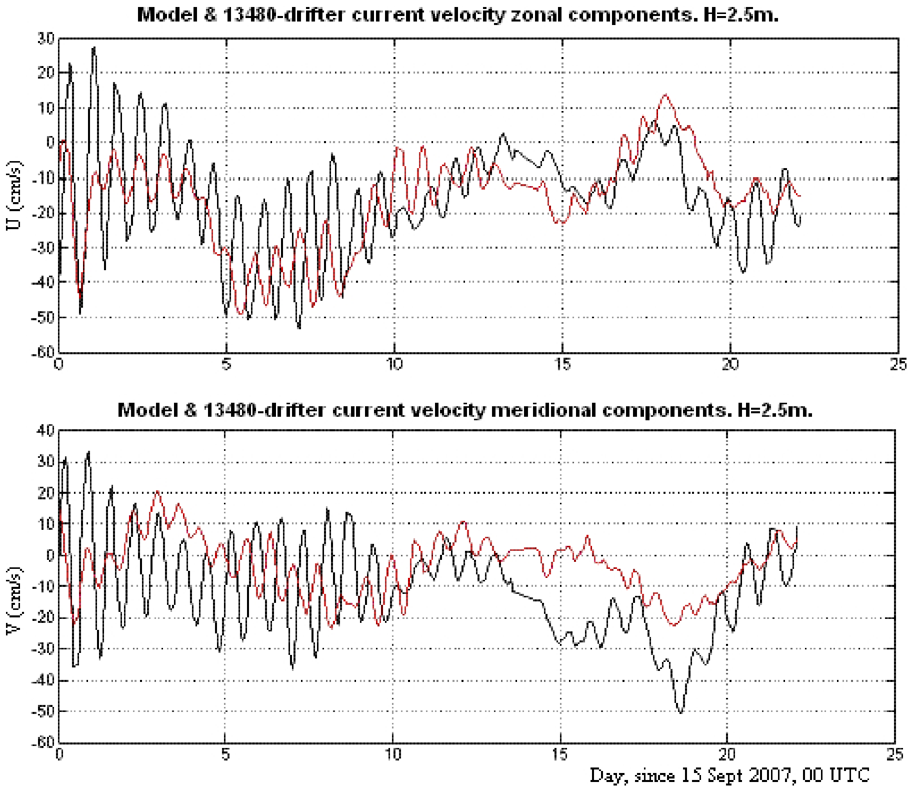

Fig. 13. Comparison of the measured (black) and simulated (red) inertial oscillations.

OSD
8, 917–954, 2011

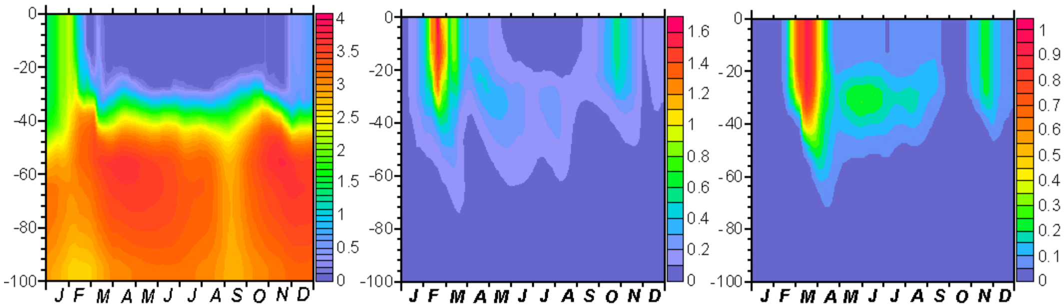

Fig. 14. Seasonal cycle of averaged over the basin area nitrates (left panel), phytoplankton (central panel) and zooplankton (right panel).

OSD

8, 917–954, 2011

Development of Black Sea nowcasting and forecasting system

G. K. Korotaev et al.

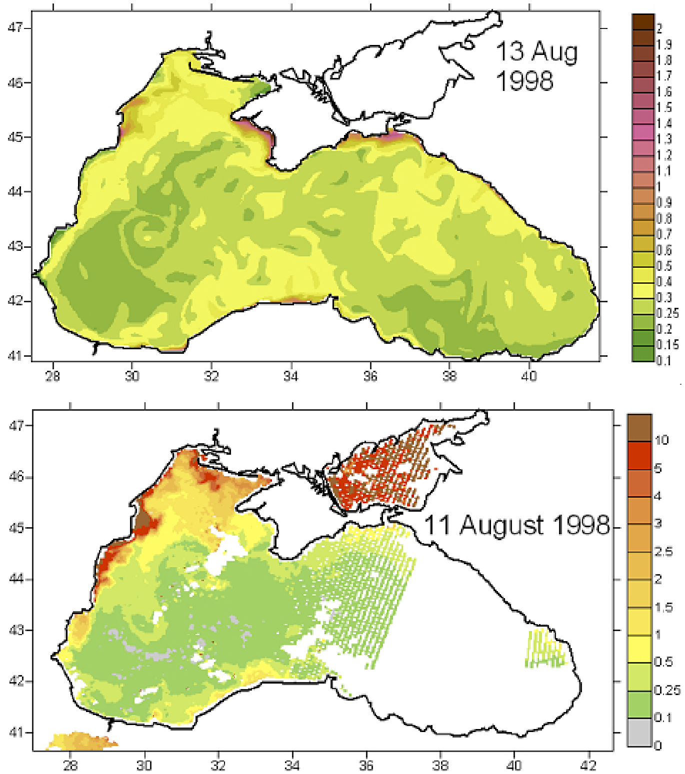

Fig. 15. Comparison of surface phytoplankton distribution in mid August 1998 simulated by the model (upper panel) with that observed by SeaWiFS spectrometer from space.

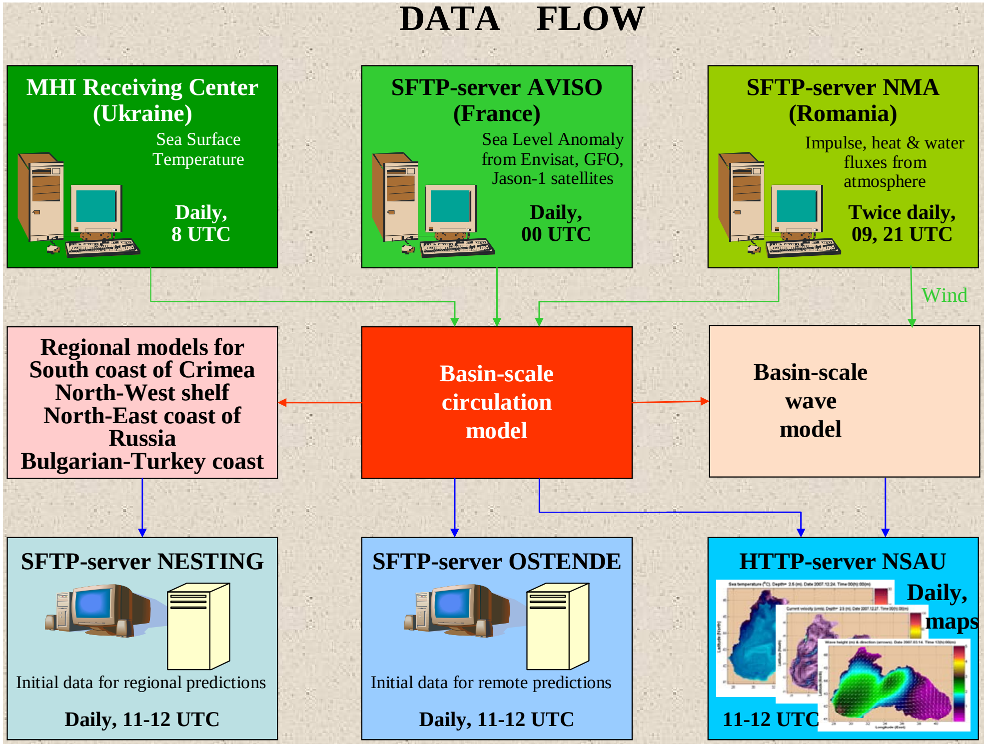

Fig. 16. Data flow in the framework of the Black Sea nowcasting/forecasting system.

OSD
8, 917–954, 2011

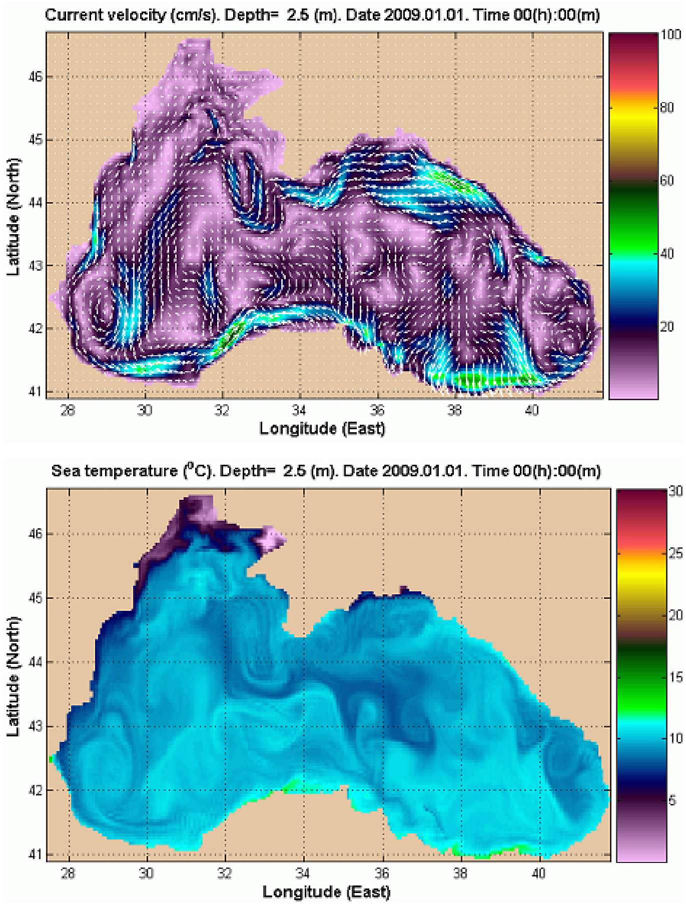

Fig. 17. Examples of the Black Sea nowcasting/forecasting system products: upper panel – surface currents, lower panel – sea surface temperature.

OSD
8, 917–954, 2011

Development of Black Sea nowcasting and forecasting system

G. K. Korotaev et al.